

Article

Soil and Nutrient Cycling Responses in Riparian Forests to the Loss of Ash (*Fraxinus* spp. L) from Emerald Ash Borer (*Agrilus planipennis*, Fairmaire)

Paul K. Sibley ^{1,*}, David Dutkiewicz ², David P. Kreuzweiser ³ and Paul Hazlett ³ ¹ School of Environmental Sciences, University of Guelph, Guelph, ON N1G 2W1, Canada² Invasive Species Center, Great Lakes Forestry Centre, Natural Resources Canada, Canadian Forest Service, Sault Ste. Marie, ON P6A 2E5, Canada; david.dutkiewicz@canada.ca³ Great Lakes Forestry Centre, Natural Resources Canada, Canadian Forest Service, Sault Ste. Marie, ON P6A 2E5, Canada; davek.636@gmail.com (D.P.K.); paul.hazlett@canada.ca (P.H.)

* Correspondence: psibley@uoguelph.ca

Received: 12 March 2020; Accepted: 23 April 2020; Published: 26 April 2020



Abstract: Emerald ash borer (EAB) is an alien invasive species that is spreading across Canada and the United States killing ash trees. In riparian forests where ash may be abundant; loss of ash can induce significant structural changes; including the creation of canopy gaps; changes in light penetration; expansion of ground vegetation; and alteration of soil nitrogen and carbon cycling. In 2014 and 2015, we examined the effects of EAB-caused gaps in riparian forests on soil nutrient dynamics. Two sites with different infestation timelines, a “new” site (mortality in past 2–3 years) and an “old” site (infested 10 years previous) were selected to determine temporal differences in effects of canopy gaps created by ash loss on litterfall, herbaceous ground vegetation, and soil nutrient cycling. Within both sites, plots with clustered dead ash (canopy gap plots—CG) were paired with nearby plots of full canopy and no ash (canopy closed plots—CC), and differences between paired plots determined. Total litterfall was observed at all sites but was only significant at the new infestation site. Reductions in leaf litter deposition in CG plots resulted in reduced N and C flux to the forest floor but soil C and N concentrations, and nitrogen mineralization rates, were not significantly different between CG and CC plots. Nitrate concentration in soil solution was significantly greater in CG plots compared to CC plots at the new infestation sites but showed the opposite trend at the old infestation sites. Herbaceous ground vegetation biomass was significantly greater (up to 10×) in CG plots than in CC plots. Overall, despite changes to riparian forest canopy structure and litterfall, there was no significant difference in soil nutrient cycling between EAB-induced canopy gaps and closed canopy plots after 10 years, suggesting a high resilience of riparian forest soils to EAB infestation

Keywords: *Agrilus planipennis*; *Fraxinus*; riparian forest; canopy

1. Introduction

The ecological function of healthy riparian forest ecosystems is governed by a dynamic relationship between biotic and abiotic components [1]. Disturbances by invasive species can disrupt the balance of functioning riparian forests by altering important biological and biogeochemical components [2]. Emerald Ash Borer (EAB), *Agrilus planipennis* Fairmaire (Coleoptera: Buprestidae) is an invasive host-specific alien species that attacks and kills healthy ash trees. First discovered in North America in 2002 near the Detroit, Windsor area [3,4], EAB is now firmly established in over 30 states, Ontario, and parts of southern Quebec [5] and is, as predicted, presenting significant research and regulatory challenges [6].

Ash trees (*Fraxinus* spp.) are commonly found in riparian forests and forested wetlands where they can be a dominant species. Mortality of ash trees in riparian forests is of great concern due to the intimate role that these ecotonal forests play in mediating the flow of energy and materials to adjacent waterbodies and potentially the functioning of headwater streams whose metabolism is intimately influenced by autochthonous subsidies from terrestrial ecosystems [7–9]. Studies examining the impacts of ash loss in riparian terrestrial ecosystems are generally poorly represented in the literature, particularly in relation to soil nutrient dynamics. Studies in upland (non-riparian) forest systems have investigated the effects of ash mortality on soil chemistry. Flower et al. [10] showed that ash loss in forests had a negative effect on carbon (C) cycling and net primary production but that this trend was partially compensated for by enhanced growth of other trees such as maple and elm. Matthes et al. [11] found that loss of ash to emerald ash borer did not affect soil microclimate or soil carbon fluxes which they attributed to the presence of well-drained, sandy soils and a diffuse distribution of ash in the forest. Neither of these studies were conducted exclusively in riparian forests and the opposing trends suggest that factors regulating soil nutrient cycling in relation to ash loss are complex.

Nisbet et al. [8] hypothesized that loss of ash in streamside riparian areas would yield a cascade of effects that could affect soil biogeochemistry. Specifically, ash mortality and subsequent reductions in ash litterfall, and the associated flux of nutrients to the forest floor could have a direct effect on nutrient inputs to the soil. For example, decreased nitrogen (N) inputs through the loss of ash leaf litter, combined with less N uptake from the soil because of ash mortality, could result in a redistribution of N in the ecosystem. Recent studies have begun to test this hypothesis. For example, Kreuzweiser et al. [12] found that EAB-induced loss of ash trees in streamside riparian forests infested at different times (\approx 5-year difference between initial infestations), significantly increased canopy openness, reduced litterfall and composition, and increased ash regeneration densities and stand structure. This, in turn, resulted in consistently and often significantly reduced C and macro-nutrient (N, phosphorus (P) potassium (K), and calcium (Ca)) flux to the forest floor. A recent study by Engelken et al. [13] assessed overstory trees, regeneration, herbaceous plants, coarse woody debris, and photosynthetically active radiation in Michigan riparian forests infested with EAB, also at different times. The canopy gaps resulting from the loss of ash trees (>85%) increased the amount of light reaching the forest floor leading to significant increases in herbaceous vegetation which decreased ash sapling regeneration. However, neither of these studies investigated the implications of the observed changes on soil nutrient dynamics.

Two recent studies, conducted in black ash dominated wetlands, have provided some insights into potential effects of ash loss on soil chemistry. Simulating ash mortality by girdling and/or cutting ash trees in a wetland in northern Michigan, Davis et al. [14] predicted an increase in soil N due to reduced uptake by the depleted vegetation but found that soil N availability was not affected. Toczydlowski et al. [15], also working in a black ash dominated wetland system in Minnesota, also simulated ash mortality by logging and girdling trees. They found little evidence that ash mortality affected overall N mineralization rates in the short term but suggested that N cycling could shift from being NO_{2+3} -centered to being NH_4^+ -centered potentially influencing microbial communities and plant uptake.

Building on the study of Kreuzweiser et al. [12], in the present study we examined the impact of canopy gap formation due to ash mortality on C and nutrient fluxes to the forest floor via litterfall, development of understory vegetation biomass, and soil nutrient cycling in streamside riparian areas. The study was conducted in riparian forests that had been infested by EAB in the previous 1–3 years (recent infestation) and in forests infested 8–10 years previously (old infestation). Our objective was to determine if gaps created by EAB in riparian forests disrupted the nutrient fluxes and cycling in soils in canopy gap (CG—gaps caused by ash mortality) locations compared to closed canopy (CC—minimal ash present) areas. We compared open canopy areas (CG) with closed canopy areas (CC) by: (1) quantifying the percentage of open canopy, (2) determining the mass of litterfall deposited on the forest floor, (3) measuring the nutrient concentrations and fluxes of litterfall deposited on the forest floor, (4) determining the biomass and nutrient content of herbaceous vegetation, and (5) determining

soil N mineralization and soil solution N concentrations. We hypothesized that riparian plots with canopy gaps (CG) resulting from the loss of ash trees compared to closed canopy (CC) plots would (1) have lower litterfall deposition; (2) increased light penetration to the forest floor; (3) reduced C and N flux to the forest floor; (4) increased understory herbaceous vegetation biomass and nutrient content; and (5) greater soil N mineralization and soil solution N concentrations. For each of these endpoints, we further expected greater differences between CG and CC plots in the old infestation compared to the new infestation due to the longer time since canopy gap formation. Similar to Engelken et al. [13], by examining both new and old infestations, we were able to compare temporal differences in forest canopy, litterfall, herbaceous vegetation, and soil nutrient cycling conditions resulting from gaps created by ash mortality.

2. Methods and Materials

2.1. Study Areas and Riparian Forest Composition

Paired plots (5×5 m) were established at each of two sites in Southwestern Ontario distinguished by differences in the timeline of infestation. The “old” infestation site (8–10 years since complete ash mortality) was located near Essex, Ontario ($42^{\circ}10'23''$ N, $81^{\circ}46'12''$ W); the “new” infestation site (1–3 years since complete or nearly complete ash mortality) was located near Glencoe, Ontario ($42^{\circ}44'50''$ N, $81^{\circ}42'34''$ W), approximately 90 km to the northeast (Figure 1). Site selection was not random insofar as we wanted to ensure a clear demarcation between closed and open canopy plots and congruence with previously published work [11]. Initial site selection was made by remote sensing (satellite images obtained from Google Earth™) followed by ground surveys. Site selection at the old site occurred after infestation had occurred whereas site selection at the new site occurred before infestation was evident. At both sites, selection was based on the following criteria: (1) the riparian forest in satellite images appeared intact and contiguous for at least 400 m in length and 30 m in width on each side of a distinct stream channel, (2) the riparian forest contained clusters of living ash in the new infestation and dead ash in the old infestation as determined from the ground surveys, (3) there was no indication of cattle grazing or other disturbances in the riparian areas, (4) the sites were reasonably accessible by road, and (5) permission to access was granted by landowners. The old infestation had five paired plots (10 plots in total) across four sites, and the new infestation had nine paired plots (18 plots in total) across five sites, all established in riparian areas such that one plot was situated directly in the center of a canopy gap (CG) area created by a cluster of dead ash, and the second plot in a nearby closed canopy (CC) area (little or no ash), approximately 25 m apart. The comparison of stands with dead ash versus non-ash stands was necessitated by the fact that no live ash remained (>90% mortality) at either site at the time the study was initiated.

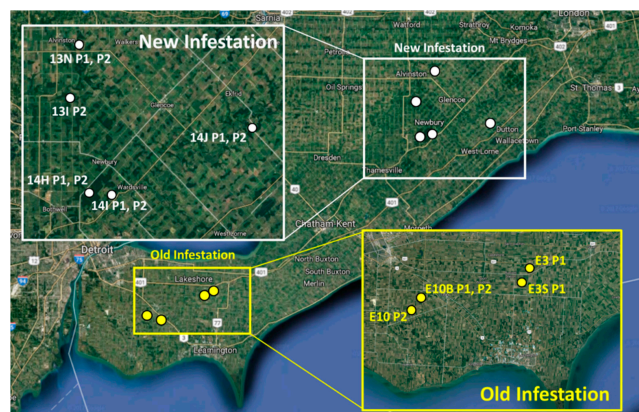


Figure 1. Locations of the 14 paired plots at the old and new infestation sites in Southwestern Ontario. Each site had two sets of paired plots spaced 50–100 m apart and, in all but one case, situated on opposite sides of the stream.

2.2. Canopy Analysis

Canopy openness was measured in the CC and CG plots from digital photographs taken in the center of each plot with a Canon EOS 50D camera, 185° SuperFisheye (5.6 mm F/5.6) lens, and a self-leveling mount on a tripod (Régent Instruments Inc.). The photos were taken during mid-day hours (approximately 1100–1500 h) over a 3-day period during full leaf out conditions (July 2015). The canopy photographs were then digitally analyzed using the software WinSCANOPY 2009a for Canopy Analysis (Régent Instruments Inc.). Consistent photo color classification was used throughout the analysis to facilitate comparisons among plots.

2.3. Litterfall

Litterfall was collected in the fall of 2014 using four plastic 34 × 38 cm litter collection containers per plot (Figure 2A). Samples were collected twice, in mid-October at approximately 50% litterfall and in early December at 100% litterfall. The four collection containers were pooled within each plot and across the two collection periods to better represent the variety of trees/shrubs throughout the plots. Litterfall samples were frozen at $-2\text{ }^{\circ}\text{C}$ prior to sorting. After thawing, the litter was separated by tree genera into leaves, shrubs, and coarse materials (twigs, seeds/nuts, bark, and petioles), dried at $70\text{ }^{\circ}\text{C}$ for 24 h, and weighed. All litter components were ground to a uniform particle size (1 mm^2) using a Wiley Mill. Total carbon and nitrogen concentrations were determined using a NCS combustion analyzer (Vario EL III, CHNOS Elemental Analyzer, Elementar Americas Inc. Mt. Laurel, NJ, USA).

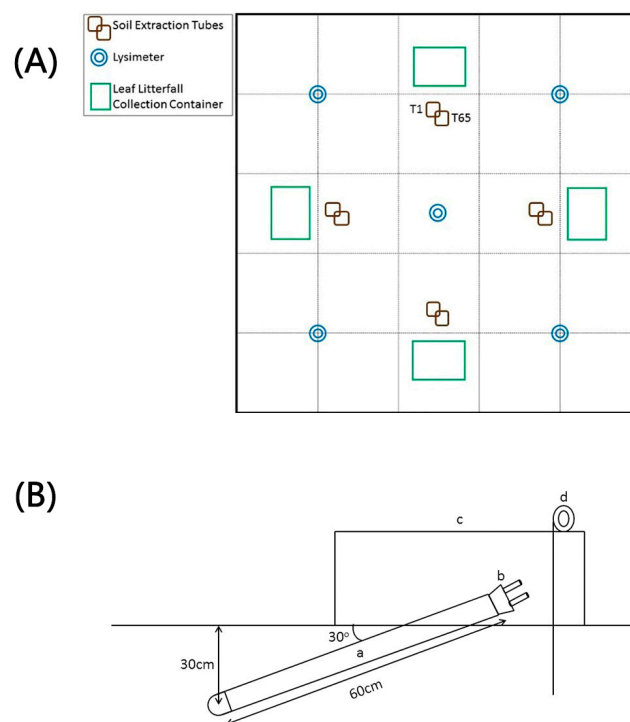


Figure 2. (A) Canopy Closed plots (CC) and Canopy Gap plots (CG) plots (5 × 5 m layout) showing the placement of soil sampling locations (incubation tubes), lysimeters, and litter collection containers. (B) Tension lysimeter system used for the extraction of water from the soil showing (a) a lysimeter with porous clay cup at a depth of 30 cm; (b) a rubber stopper with sealable air and soil solution extraction ports; (c) above-ground cover to protect the exposed portion of the lysimeter; and (d) a pigtail pin to keep the cover in place.

2.4. Herbaceous Ground Vegetation

Herbaceous ground vegetation was collected at the end of July 2015 when the vegetation was in full leaf. A 1 × 1 m quadrat was placed near the center of each plot to collect all the non-woody

vegetation. All herbaceous vegetation in the 1 m² quadrat was clipped at ground level with shears and transferred to a paper bag for storage. Prior to analysis, the samples were dried at 70 °C for 24 h and weighed to obtain total biomass. The combined samples (elemental measurements were not conducted on a specific-specific basis for herbaceous vegetation) were processed and analyzed for C and N as described for the litterfall samples.

2.5. Soil N Mineralization

Soil N mineralization in CC and CG plots was evaluated using two methods: in-situ core incubations [16] and anaerobic laboratory incubations [17]. For the in-situ incubations, at each of four locations in each CC and CG plot (Figure 2A), two PVC soil incubation tubes (5 cm diameter and 20 cm length) were hammered vertically into the soil in early June (9th–14th) of 2015 until the tubes were flush with the soil surface. One tube was covered and remained in the soil for 65 days. The second tube was removed immediately and refrigerated at 4 °C (hereafter T1). After 65 days (T65), the remaining in situ tube was removed and refrigerated (4 °C). The soil from each tube was extruded and the 0–10 cm depth (Ah horizon) was sampled from the core and passed through a 2 mm sieve to remove roots and coarse fragments and to create a homogenized sample. A subsample (1 g) of soil was taken from each of the T1 and T65 samples to determine moisture content by drying for 24 h at 110 °C. To measure inorganic N (NH₄⁺-N and NO₃⁻-N), 20 g oven-dried equivalent weight samples from each T1 and T65 tubes were weighed into 120 mL glass vials and shaken for 1 h with 60 mL of 2 M KCl. The samples were filtered (0.45 µm) and analyzed for inorganic N using a Technicon autoanalyzer IIC using sodium nitroprusside and cadmium reduction methods [18].

For the laboratory incubations, field moist subsamples of soil collected from each CC and CG plot at T1 were anaerobically incubated to determine potential mineralizable N. Then, 20 g oven-dried equivalent weight samples were weighed into 120 mL glass vials and shaken for 1 h with 60 mL of 2 M KCl solution. A second 20 g sample was weighed into a 120 mL glass vial and incubated in the dark for 14 days at 30 °C after addition of 30 mL distilled/deionized water. At the conclusion of the incubation period, the samples were shaken for 1 h with 30 mL of 4 M KCl solution. As above, samples were filtered, and the extracts analyzed for NH₄⁺-N using the sodium nitroprusside method on a Technicon autoanalyzer IIC. Accumulation or depletion of inorganic-N during the field and laboratory incubations was calculated by subtracting initial from final concentrations.

Finally, a subsample of soil from each CC and CG plot sampled at T1 was air-dried, ground (Fritsch, Planetary Mono Mill Pulverisette 6), and placed into 4-dram glass vial for analysis. C and N concentrations were determined using a combustion analyzer (Vario EL III, CHNOS Elemental Analyzer for Elementar Americas Inc. Mt. Laurel, NJ, USA).

2.6. Soil Solution

Five porous cup tension lysimeters were used to collect soil solution in each CC and CG plot (Figure 2A). Lysimeters (60 cm in length) were installed at a 30° angle to allow the porous clay sampling point to sit approximately 30 cm below the soil surface (Figure 2B). The holes were bored using a soil auger and a 30° wooden angled jig to maintain consistency across plots. Tension in the lysimeters was set at -50 kPa using a hand vacuum pump with pressure gauge. Samples were collected every 4 weeks (June–December 2014, April–July 2015) for a full calendar year excluding January–March. Negative pressure was maintained in >90% of lysimeters between sampling periods. Samples were bulked between the five lysimeters in each plot at each sampling date using a 2000 mL graduated cylinder; lysimeters in which tension was lost were not included in the bulk samples. Lysimeter samples were stored on ice in the field and refrigerated at 4 °C until processing and analysis. All samples were analyzed within 48 h of collection. All samples were initially filtered through a coarse mesh filter (Fisher quantitative Q8 filter paper) and then passed through a 0.45 µm paper filter prior to analysis. Inorganic N (NH₄⁺-N and NO₃⁻-N) and total N were determined on a Technicon autoanalyzer IIC using sodium nitroprusside, cadmium reduction and autoclave digestion-cadmium reduction methods, respectively.

2.7. Statistical Analysis

Paired *t*-tests were applied to each endpoint to test for differences between the CG and the CC plots within the new and old infestations. We anticipated differences due to infestation age (older infestation would have greater effects), so data from the new and old infestations were analyzed separately. Differences between CG and CC plots in litterfall mass and nutrient concentrations were tested separately for leaves of each tree genus, shrubs, and coarse material (twigs, seeds/nuts, bark, and petioles). For all analyses, data were \log_{10} transformed to ensure that the assumptions of normal distribution and homogeneity of variance were met.

The nutrient flux of each leaf genera, shrub, and coarse material was calculated by using the mass (kg ha^{-1}) of the leaves collected multiplied by the nutrient concentration (ppm). The same approach was used to determine nutrient content of herbaceous ground vegetation. Differences in all nutrient-related measurements (litterfall C and N concentrations and flux, herbaceous vegetation C and N concentrations and content, soil and soil solution C and N concentrations, and soil and lab incubation inorganic N concentrations) between CG and CC plots were analyzed using paired *t*-tests. All tests were conducted using SigmaPlot for Windows Version 12.0 (Build 12.0.0182 Copyright© 2020 Systat Software, Inc., San Jose, CA, USA) and a significance level of 0.05 was used.

3. Results

3.1. Canopy Analysis

Mean percent openness of canopy in CG plots was significantly greater in both new ($p = 0.002$; Figure 3A) and old ($p = 0.03$; Figure 3B) infestations. Mean percent canopy openness in the old infestation sites was 28% and 13% for CG and CC plots, respectively, compared to 15% and 10% for the new infestation sites. Canopy openness varied between 8% and 21% across both plot types in the new infestation sites compared to 6–44% in old infestation sites, reflecting the greater proportion of dead ash trees that had fallen in CG plots at old infestation site compared to CG plots at the new infestation site where dead ash were still standing.

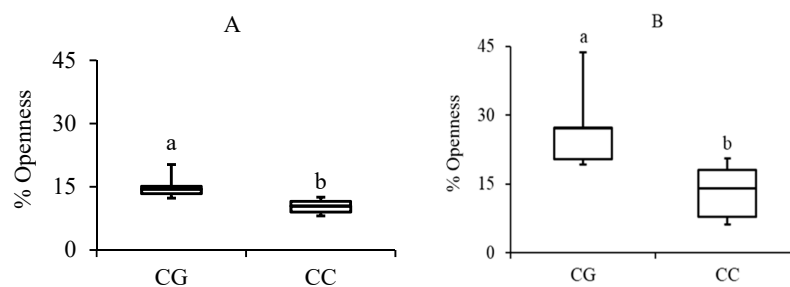


Figure 3. Percent openness for Canopy Gap (CG) plots and Canopy Closed (CC) plots for the new (A) and old (B) infestation sites. Boxes represent the 25th and 75th quartiles, and the horizontal line the median. The whiskers represent the maximum and minimum average plot values for the sites. Boxes with different letters indicate significant differences between the sites (Student's *t*-test: new $p = 0.002$, old $p = 0.03$).

3.2. Litterfall Deposition

With the exception of maple, there were no significant differences in leaf litterfall among tree genera between CG and CC plots at either infestation (Table 1). Maple was the most abundant leaf litter type in all plots (roughly twofold or greater than other contributors), and its deposition was significantly lower in CG than in CC plots for both infestations. Ash, predominantly from regenerating saplings, comprised a low percentage of leaf litterfall compared to other tree species and was not significantly different between CC and CG plots at either site. Similar to the maple leaf litter, total litterfall was significantly ($p = 0.04$) greater in CC plots compared to CG plots but only in the new

infestation site. Deposition of coarse material (twigs, bark, seeds/nuts, and petioles) was consistently greater in CC plots compared to CG plots, but estimates were highly variable and the differences not significant (Table 1).

Table 1. Mean (\pm SEM) litter deposition (kg ha^{-1}) for Canopy Gap (CG) plots and Canopy Closed (CC) plots in new and old infestation sites.

Genus	New					Old				
	CG kg ha^{-1}		CC kg ha^{-1}		<i>p</i> -Value	CG kg ha^{-1}		CC kg ha^{-1}		<i>p</i> -Value
<i>Fraxinus</i> spp.	46	(19)	32	(14)	0.41	36	(22)	4	(3)	0.53
<i>Acer</i> spp.†	720	(230)	1132	(226)	0.02 *	1691	(431)	2134	(512)	0.02 *
<i>Carya</i> spp.	377	(132)	537	(194)	0.21					
<i>Fagus</i> sp.	132	(26)	255	(111)	0.28					
<i>Juglans</i> sp.	351	(79)	306	(90)	0.66	495		1030		
<i>Ostrya</i> sp.	57	(17)	94	(24)	0.35	78		1		
<i>Populus</i> spp.	112	(77)	355	(196)	0.59	26	(14)	22	(2)	0.46
<i>Quercus</i> spp.	383	(183)	401	(142)	0.85	404	(102)	466	(357)	0.68
<i>Tilia</i> sp.	129	(43)	210	(82)	0.27					
<i>Ulmus</i> spp.	330	(140)	308	(132)	0.69	257	(99)	585	(267)	0.38
Shrub	377	(98)	197	(69)	0.06	149	(41)	181	(118)	0.75
Coarse material	462	(49)	547	(85)	0.38	650	(250)	778	(308)	0.80
Total†	3476	(58)	4375	(83)	0.04 *	3785	(151)	5201	(199)	0.18

† Data was \log_{10} transformed; **bold**—only one site was found to have this tree species. * Significant differences between CG and CC (Student's *t*-test).

3.3. Litterfall Elemental Concentrations and Flux to Forest Floor

For both the new and old infestation sites, N concentrations in leaf litter for all tree genera were not significantly different between CG and CC plots (Figure 4A,B) except for elm (*Ulmus* spp.) which had higher N concentrations ($p = 0.006$) in CG plots at the new infestation sites. Among the remaining genera, N concentrations tended to follow similar patterns with slightly greater N in CG than CC plots in the new infestation and slightly lower in CG than CC plots in the old infestation. Average C concentrations in leaf litter also did not differ between CG and CC plots among sites except for ironwood (*Ostrya* sp.) which had significantly greater ($p = 0.01$) C concentration in the CG plots of the new infestation (Figure 4C,D). While the remaining genera were not significantly different, there tended to be greater average C concentrations in leaf litter in CG plots versus CC plots in both infestations. Leaf litter C:N ratio ranged from the smallest in the new infestation for elm, 27 (± 2), to greatest for beech (*Fagus* sp.), 72 (± 3). In the old infestation, leaf litter C:N ratio ranged from 32 (± 2) for both ash and walnut (*Juglans* sp.) to 65 (± 4) for beech. There were no significant differences between the CG and the CC plots with the exception of elm ($p = 0.002$) which had a lower C:N ratio in the CG plots (Figure 4E,F).

In terms of litter-derived N flux to the forest floor, the only genus that differed between CG and CC plots was maple which was significantly lower ($p = 0.03$) in CG plots of the new infestation. N flux from total litterfall was lower, though not significantly so, in CG plots of the new infestation and was significantly lower in CG plots of the old infestation ($p = 0.03$) (Table 2). Similarly, the flux of C from maple litter was significantly lower ($p = 0.01$) in the CG plots of the new infestation and about 20% lower in CG plots of the old infestation although differences in the old infestation were not significant (Table 3). C flux from all other genera was not significantly different between CG or CC plots for new and old infestations. However, C flux from total litterfall was significantly lower in CG plots in both the new ($p = 0.02$) and old ($p = 0.03$) infestations.

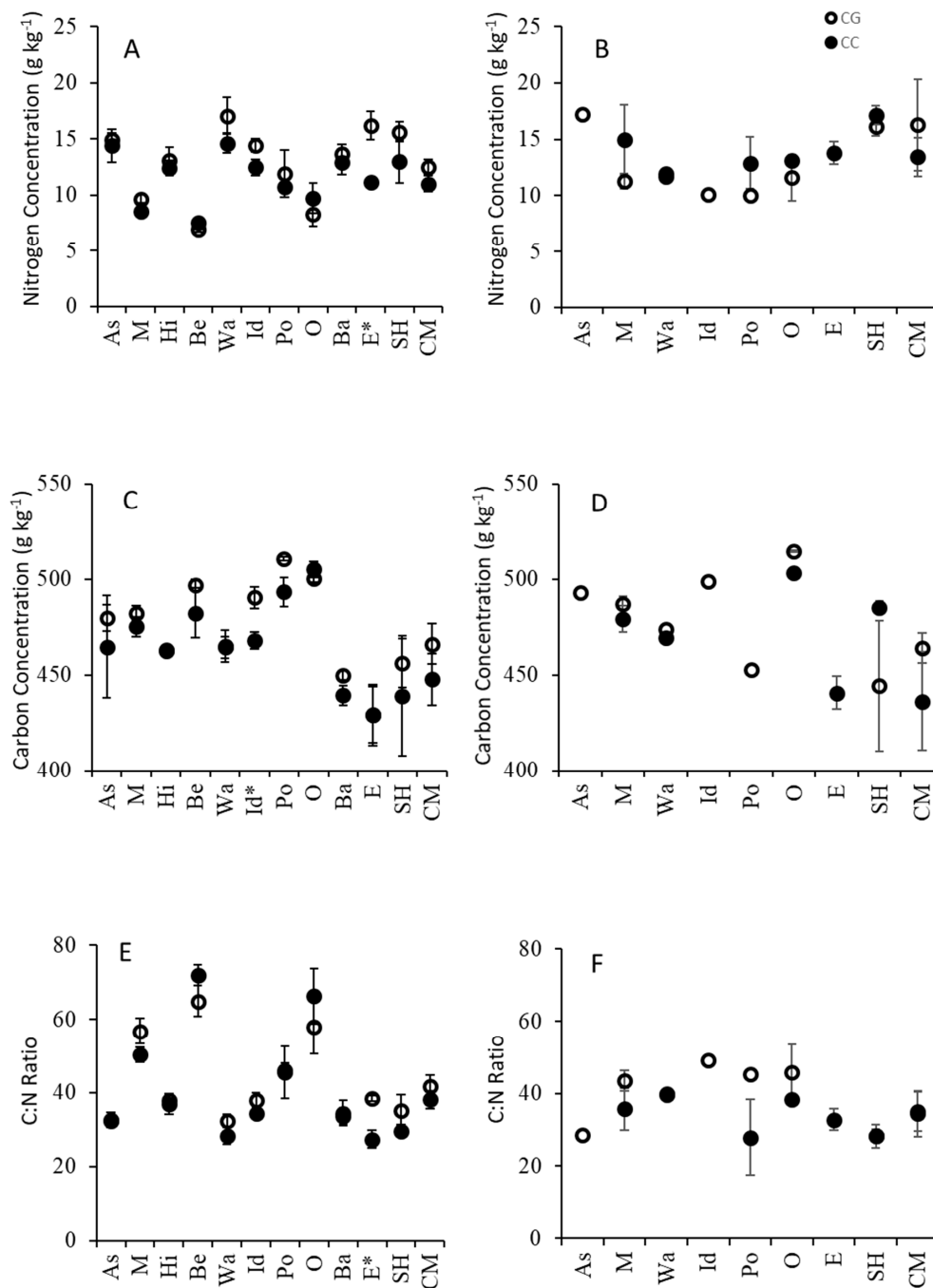


Figure 4. Mean (\pm standard deviation) leaf litter nitrogen (A,B) and carbon (C,D) concentrations ($g\ kg^{-1}$) and C:N ratio (E,F) in the new (left-hand plots) and old (right-hand plots) infestations. Asterisk indicates tree genera with significant difference in nitrogen concentration ($p < 0.05$) between Canopy Gap (CG) plots and Canopy Closed (CC) plots (Student's t -test: (A) elm $p = 0.009$, (C) ironwood $p = 0.015$, (E), elm ($p = 0.004$). As (Ash—*Fraxinus*), M (Maple—*Acer*), Hi (Hickory—*Carya*), Be (Beech—*Fagus*), Wa (Walnut—*Juglans*), Id (ironwood—*Ostrya*), Po (Polar—*Populus*), O (Oak—*Quercus*), Ba (Basswood—*Tilia*), E (Elm—*Ulmus*), SH (shrub), CM (Coarse Material).

Table 2. Mean (\pm SEM) N flux of leaf litterfall (kg/ha^{-1}) in the Canopy Gap (CG) plots and Canopy Closed (CC) plots for the new and old infestation sites.

	New					Old				
	CG kg ha^{-1}		CC kg ha^{-1}		<i>p</i> -Value	CG kg ha^{-1}		CC kg ha^{-1}		<i>p</i> -Value
<i>Fraxinus</i> spp.	0.9	(0.4)	1.0	(0.1)	0.67	1.2				
<i>Acer</i> spp.†	7.2	(2.4)	10.0	(2.0)	0.03 *	18.6	(5.4)	28.0	(4.5)	0.30
<i>Carya</i> spp.	5.1	(2.0)	7.3	(2.4)	0.37					
<i>Fagus</i> sp.	0.9	(0.3)	2.5	(1.4)	0.29					
<i>Juglans</i> sp.	5.8	(1.6)	4.8	(1.8)	0.45	5.9		12.1		
<i>Ostrya</i> sp.	1.3	(0.2)	1.5	(0.2)	0.56	0.8				
<i>Populus</i> spp.	3.7	(2.9)	6.4	(4.1)	0.70	0.6		4.0		
<i>Quercus</i> spp.	4.5	(2.6)	5.0	(2.0)	0.81	5.0	(2.7)	18.2		
<i>Tilia</i> sp.	1.9	(0.9)	3.6	(1.8)	0.47					
<i>Ulmus</i> spp.	5.0	(2.5)	3.9	(1.7)	0.72			8.3	(4.1)	
Shrub	5.9	(1.7)	4.2	(0.6)	0.36	2.4	(0.7)	7.7	(3.0)	0.30
Coarse material	5.7	(0.6)	6.1	(1.1)	0.73	9.6	(3.7)	9.1	(3.6)	0.90
Total †	47.9	(0.6)	56.3	(0.7)	0.08	44.1	(2.2)	87.4	(2.9)	0.03 *

† Data was \log_{10} transformed, **bold**—only one site was found to have this tree species, * significant differences between CG and CC (Student's *t*-test).

Table 3. Mean (\pm SEM) C flux of litterfall (kg ha^{-1}) in the Canopy Gap (CG) plots and Canopy Closed (CC) plots for the new and old infestation sites.

	New					Old				
	CG kg ha^{-1}		CC kg ha^{-1}		<i>p</i> -Value	CG kg ha^{-1}		CC kg ha^{-1}		<i>p</i> -Value
<i>Fraxinus</i> spp.	27.2	(10.1)	35.6	(3.2)	0.46	35.4				
<i>Acer</i> spp.†	347.6	(110.6)	539.4	(108.2)	0.01 *	825.6	(275.9)	1031.9	(285.8)	0.63
<i>Carya</i> spp.	175.5	(65.8)	282.5	(94.2)	0.18					
<i>Fagus</i> sp.	65.6	(18.1)	151.9	(75.7)	0.29					
<i>Juglans</i> sp.	163.6	(43.1)	144.2	(49.5)	0.67	234.4		483.6		
<i>Ostrya</i> sp.	42.9	(6.4)	56.2	(10.2)	0.30	39.1				
<i>Populus</i> spp.	129.5	(88.9)	285.5	(176.2)	0.55	27.5		195.5	(194.3)	
<i>Quercus</i> spp.	221.2	(102.7)	231.9	(76.9)	0.84	207.8	(83.0)	698.0		
<i>Tilia</i> sp.	58.1	(24.4)	123.5	(58.6)	0.39					
<i>Ulmus</i> spp.	136.1	(67.6)	148.9	(63.2)	0.89			262.2	(123.2)	
Shrub	172.0	(47.2)	151.7	(31.8)	0.73	67.2	(19.9)	214.3	(73.6)	0.28
Coarse material	214.0	(20.4)	251.0	(45.3)	0.43	304.2	(116.9)	356.7	(146.9)	0.82
Total	1753.2	(26.4)	2402.1	(38.6)	0.02 *	1741.2	(94.6)	3242.1	(108.4)	0.03 *

† Data was \log_{10} transformed, **bold**—only one site was found to have this tree species, * significant differences between CG and CC (Student's *t*-test).

3.4. Herbaceous Ground Vegetation

The total biomass of herbaceous ground vegetation was significantly greater in CG than in CC plots of both infestations, particularly in the old infestation sites where herbaceous biomass in CG plots was $\approx 10\times$ higher than in CC plots (Table 4). N and C concentrations and C:N ratio in herbaceous vegetation at the new infestation was not significantly different between CG and CC plots (Table 4). However, the N concentration was significantly ($p = 0.01$) lower in herbaceous ground vegetation in CG plots at the old infestation site compared to CC plots, leading to significantly higher C:N ratio in the CG plots (Table 4). Owing to the higher biomass in CG plots, total N and C content in herbaceous vegetation was significantly greater in the CG plots compared to CC plots (Table 4).

Table 4. Mean (\pm SEM) biomass (kg ha^{-1}), N and C concentrations (g kg^{-1}), C:N ratio, and the N and C nutrient content (kg ha^{-1}) of herbaceous ground vegetation in Canopy Gap (CG) plots and Canopy Closed (CC) plots at the new and old infestation sites.

Measure	New			Old		
	CG	CC	<i>p</i> -Value	CG	CC	<i>p</i> -Value
Biomass	657 (115)	105 (22)	<0.001 *	2653 (613)	259 (79)	0.01 *
N concentration	21 (1)	22 (10)	0.60	13 (1)	23 (2)	0.01 *
C concentration	431 (16)	408 (16)	0.24	396 (21)	329 (36)	0.05
C:N ratio	21 (1)	20 (2)	0.36	31 (4)	14 (2)	0.01 *
Total N content	13 (2)	2 (1)	<0.001 *	35 (9)	6 (2)	0.016 *
Total C content	283 (50)	43 (9)	<0.001 *	1005 (169)	78 (19)	0.005 *

† Data was \log_{10} transformed, * significant differences between CG and CC (Student's *t*-test).

3.5. Soil C and N and N Mineralization

Soil C and N concentrations and C:N ratio in the surface mineral soil (0–10 cm) were not significantly different between CG or CC plots at either infestation site (Table 5). In soils of the old infestation CG plots, a small net increase in NH_4^+ -N was observed; however, there was a corresponding depletion of NO_3^- -N, resulting in a net immobilization of total inorganic-N during the 65-day incubation period. Nitrate accumulation occurred in both CG and CC plots at the new infestation sites but not at the old infestation sites. The laboratory incubation results indicated no significant differences in the amount of NH_4^+ -N between CG and CC plots in either the new or old infestations.

Table 5. Mean (\pm SEM) chemical properties of surface (10 cm; Ah horizon) soil sampled from Canopy Gap (CG) plots and Canopy Closed (CC) plots at the new ($n = 9$) and old ($n = 5$) infestation sites used for in-situ and laboratory incubation experiments.

	C (g kg^{-1})		N (g kg^{-1})		C:N	N Mineralized (65-day In-Situ Incubation)			N Mineralized (14-day Anaerobic Lab Incubation)	
						NO_3^- -N ($\mu\text{g g}^{-1}$)	NH_4^+ -N ($\mu\text{g g}^{-1}$)	Inorganic N ($\mu\text{g g}^{-1}$)	NH_4^+ -N ($\mu\text{g g}^{-1}$)	
New (CG)	4.21 (0.23)	0.33 (0.01)	12.56 (0.46)	1.83 (0.83)	−0.05 (0.02)	1.77 (0.82)	6.15 (0.42)			
New (CC)	4.25 (0.29)	0.34 (0.02)	12.66 (0.58)	1.87 (1.42)	−0.06 (0.13)	1.81 (1.38)	8.55 (1.33)			
Old (CG)	4.99 (0.28)	0.45 (0.02)	10.99 (0.67)	−0.69 (0.83)	0.09 (0.04)	−0.60 (0.84)	4.65 (0.55)			
Old (CC)	4.80 (0.37)	0.44 (0.01)	10.81 (0.64)	0.59 (1.33)	0.03 (0.06)	0.62 (1.31)	5.39 (0.64)			

3.6. Soil Solution

Mean annual NO_3^- -N, total inorganic N, and total N concentrations in soil solution were significantly greater in CG soils in the new infestation sites compared to the CC plots (Table 6). The opposite relationship was observed in the old infestation site soils, with NO_3^- -N, inorganic N, and total N concentrations being significantly lower in CG plots compared to CC plots. Soil solution NH_4^+ -N concentrations were not significantly different between CG and CC plots in both new and old infestation sites. Total N and NO_3^- -N concentrations in soil solution were greatest in July and August 2014, especially at the new infestation sites, and generally declined thereafter, except for a second, smaller peak increase in April 2015 during the snowmelt period (Figure 5A–D). NH_4^+ -N concentrations were small and variable over the study period (Figure 5E,F).

Table 6. Mean (\pm standard error) annual NO_3^- , NH_4^+ , and total N values in soil solution (mg L^{-1}) for the old and new infestations across the Canopy Gap (CG) plots and Canopy Closed (CC) plots.

		NO_3^- -N	p -Value	NH_4^+ -N	p -Value	Inorganic-N	p -Value	Total N	p -Value				
New Infestation	CG	3.44	(0.58)	<0.001	0.09	(0.04)	0.464	3.53	(0.61)	0.003	4.58	(0.72)	0.007
	CC	1.79	(0.46)		0.19	(0.11)		1.98	(0.51)		2.85	(0.59)	
Old infestation	CG	0.57	(0.17)	0.005	0.07	(0.02)	0.746	0.64	(0.17)	0.002	1.46	(0.21)	0.003
	CC	1.54	(0.29)		0.09	(0.06)		1.55	(0.24)		2.44	(0.33)	

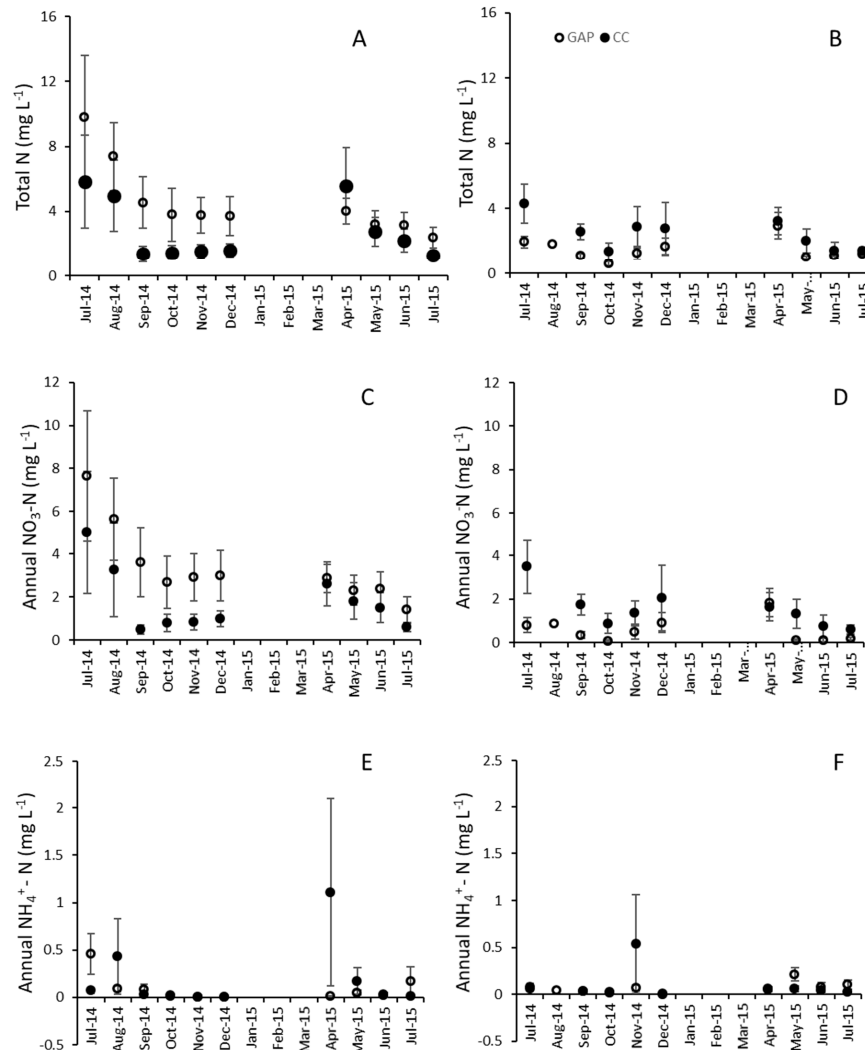


Figure 5. Mean (\pm SD) total N (A,B) NO_3^- -N (C,D), and NH_4^+ -N (E,F) concentrations (mg L^{-1}) in the soil solution at 30 cm depth. The Closed Canopy (CC) sites (closed circles) and the Canopy Gap (CG) sites (open circles) for the new (left-hand plots) and old (right-hand plots) infestations shown in the time series throughout the collection year.

4. Discussion

Clustered ash trees are commonly found in riparian areas and their loss can lead to a cascade of effects [9,12,19]. Our study demonstrated that ash mortality at both new and old infestation sites resulted in canopy gaps in areas where ash was clustered, and corresponding changes in litterfall, soil N leaching, and herbaceous plant biomass. At the new infestation sites, most ash trees remained standing with no leaf canopy over the study period compared to the old infestation sites where many trees had fallen. At the old infestation sites, we observed larger gaps and greater openness where fallen dead ash had created further site disturbance via damage to non-ash species by snapping off limbs,

crushing saplings, and breaking tree trunks. Although we did not measure photosynthetically active radiation, previous studies have documented significantly increased light penetration to the forest floor in riparian areas experiencing ash loss [13,14]. In the present study, increased light penetration would be expected given the significantly increased canopy openness and is evidenced by the significant increase in herbaceous vegetation biomass in CG versus CC plots.

At the new infestation sites, gaps created by ash mortality resulted in significantly lower total litterfall in CG plots than in CC plots; an even larger difference was observed between CG and CC plots at the old infestation plots, but the relationship was not significant due to large plot-to-plot variation. Although total litterfall was lower in CG plots overall, leaf litterfall varied between individual genera for the new and old infestations with some genera depositing more leaves in CG plots and others in CC plots. At the old infestation sites, reductions in total litter deposition to the forest floor in CG plots was not as greatly reduced as expected, likely because of increased litter inputs from adjacent living trees and shrubs. However, even by 10 years post EAB infestation and ash mortality, expansion of the existing forest canopy and seedling regeneration at the CG sites had not led to complete attenuation of litter loss. The riparian forests in this study were largely dominated by maple and ash and the contribution of maple leaves to total litterfall was greatest among tree species. In both new and old infestations, maple litter was significantly lower in the CG plots. This reflects the higher density of ash trees within the CG plots prior to EAB infestation. Maple occurred at the fringe of the canopy gaps as dictated by the clustered configuration of ash in the CG plots, whereas in the CC plots ash was scattered as an upper canopy tree amongst the maple trees which dominated the mid-to-upper canopy.

Ash leaves constituted only a small fraction of litterfall and was substantially reduced relative to the pre- or early-infestation rates (321 kg ha^{-1}) reported by Kreuzweiser et al. [12]. While ash litter was slightly greater at the new versus old infestation sites, the reduction in either case was not unexpected given the eventual complete death of the ash trees. The presence of some ash litter where all mature ash trees were dead reflected inputs from juvenile regenerating ash stems, which were particularly prevalent in CG plots [12]. This concurs with others [14,20] who have reported high rates of ash regeneration from seedlings and epicormic shoots in EAB-killed ash stands. The degree to which ash regeneration will continue to provide a source of ash litter to soils will depend on rates of re-infestation by EAB and survival of regenerating ash; based on current knowledge, it is predicted that ash will only persist in riparian areas and on the landscape in juvenile, shrub form [20]. Nevertheless, our data indicate that juvenile forms of ash will continue to provide a source of ash litter to soils. Natural canopy cover reestablishment in gaps from colonization and proliferation of species on the edge of gaps [21] would be expected to eventually eliminate the differences in total leaf litter deposition between CG and CC plots. This is supported by Kreuzweiser et al. [12] who observed consistent, though not statistically significant, increases in post-infestation leaf litterfall by maple, walnut, and hickory in riparian plots of the same study region.

We expected that EAB-induced mortality of ash trees in riparian forests would modify C and nutrient inputs to soil due to the loss of ash in litterfall reaching the forest floor and to changing proportions of leaf litter from non-ash tree species. Specifically, we hypothesized that the N concentrations in leaf litter would be elevated in non-ash genera in CG plots due to reduced N uptake by ash and hence greater soil N availability compared to CC plots. This hypothesis was only found to be true for elm leaves in the new infestation sites (Figure 4), which showed a significant increase in N concentration and corresponding reductions in C:N ratio. It is not clear why the other tree species living on the edges of the newly formed gaps did not follow the same trend in light of the competitive release through gap formation and significant increases in NO_3^- -N in CG soils at the new infestation sites (see Table 6). Elm is an early-successional species in riparian areas and may be able to respond more rapidly to changes in soil nutrient availability compared to the other genera. For example, Walters and Reich [22] found that N-content in elm leaves increased with increasing soil nitrate availability and Flower et al. [10] showed that elm had one of the highest relative growth rates among tree species in EAB-impacted forest sites. However, the lack of a similar response in the

other tree species suggests that other factors may have influenced N uptake in the CG plots at the new infestation sites. Considering that the trend of increased N concentration in elm leaf litter was not observed at the old infestation sites, it is likely that this increase was a short-term, temporary response to the gap creation.

Concentrations of N and C remained relatively unchanged in leaves across tree species, but the total flux of N and C to the forest floor was consistently, albeit not always significantly, less in CG plots due to the decrease in litterfall mass. Total litterfall N flux was not significantly different between CG and CC plots at the new infestation sites but was significantly less (approximately half) in CG plots at the old infestation. Total litterfall C flux was substantially lower in CG plots compared to CC plots in new and old infestations. In terms of specific leaf litter, only maple, the most common tree at the study sites, showed significantly lower N and C flux via leaf litter for the CG plots in the new infestation sites (a decrease was also observed at the old infestation sites but the differences were not significant). The lower C and N flux in maple in CG plots likely reflects the lower proportions of maple originally in these plots due to the clustered nature of the ash trees. Kreuzweiser et al. [12] found that leaf deposition from common tree species, including maple, increased up to 37% over a 4-year period following loss of riparian ash and Flower et al. [10] showed that the relative growth rate of non-ash species increased significantly following ash death in upland forests. Collectively, the relatively rapid compensatory changes in forest composition found in these studies indicates that changes in N and C flux to riparian soils following the loss of ash is likely to be transient.

The creation of gaps due to ash mortality yielded significantly increased understory herbaceous vegetation biomass, and increased N and C content in that vegetation, compared to the closed canopy plots. Proliferation of the herbaceous vegetation was most prevalent at the old infestation sites where CG plots had 10, 5, and 12 times more biomass, N and C content than the CC plots. More prolific vegetation growth at old infestation sites reflects the longer time since defoliation and, to a lesser extent, increased light penetration due to the larger canopy gaps once the ash trees had fallen. The significant increase in biomass of the ground vegetation in CG plots in the new and old infestation sites has been observed in other studies [20,23–25] and is consistently attributed to increased light penetration due to gap formation. Canopy openings create small micro-climates where herbaceous ground vegetation can thrive [23,26] but this process will eventually reverse as compensatory growth of non-ash species and regenerative saplings gradually close the canopy [24].

In the old infestation sites the herbaceous ground vegetation in the CG plots had lower N concentrations in the plant material, significantly increasing the C:N ratio of the ground vegetation in the CG plots. While this result may seem counterintuitive given the increased N availability in CG soil, the more rapid growth in CG plots at the old infestation may indicate dilution of the N concentration [27] within the herbaceous plant tissues. This had not yet happened at the new infestation plots because the herbaceous vegetation had not reached the degree of proliferation observed at the older sites. For example, compared to CC sites, observations at the CG plots in the old infestation indicated that a dense layer of vegetation (often including Giant Ragweed (*Ambrosia trifida* L.), which grew upwards of 2–4 m), whose growth undoubtedly contributed to the apparent dilution of tissue N concentrations. Despite tissue N concentrations being lower in the ground vegetation of the CG plots at the old sites, the total N content was almost six times greater than in the vegetation of CC plots due to the large increase in biomass. Bauhus and Bartsch [28] studied nutrient loss in forest canopy gaps and concluded that increased growth of vegetation prevented nutrient export and promoted regeneration of trees when these nutrients were cycled through decomposition. This rapid N uptake in understory vegetation may also be restricting uptake by the mature trees at the edge of gaps resulting in the lack of leaf litter N concentration response noted above. Therefore, the prolific increase in ground vegetation in gaps at the older infestation sites in our study may positively affect a critical riparian ecosystem function in that it may increase N uptake and retention in the riparian areas and recycle that N for regenerating trees, thereby reducing leaching to ground and surface water.

Contrary to our hypothesis, no differences in surface mineral soil total C and N concentrations or in soil N mineralization between CG and CC plots in new or old infestations based on in-situ and laboratory incubations. These findings agree with Davis et al. [14] who observed minimal impacts to soil N availability over a 4-year period following removal of ash via logging or girdling in ash-dominated wetland systems in northern Michigan. Further, our findings are in partial agreement with Toczydlowski et al. [15] who simulated EAB-induced ash mortality by girdling and clear-cutting black ash in northern Minnesota wetlands. In laboratory incubations, they found an order-of-magnitude increase in N mineralization overall compared to field bulk soil measurements but no differences between treatments. In contrast, in the field, they found significant differences between the treatments, with the clearcut treatment having greater overall N mineralization compared to the control and girdle treatments. These differences were attributed to changes in the microenvironment. Our findings are also consistent with similar research conducted in forests affected by hemlock woolly adelgid. For example, Jenkins et al. [29] found that infested forest areas in Southern New England were not significantly different in soil C and N compared to un-infested sites and Knoepp et al. [30] found no differences between treatments in soil C content, N mineralization rates and soil solution N concentrations over a 4-year measurement period in southern Appalachian forests. However, the results stand in contrast to those of Lovett et al. [31] who showed a decrease in soil C:N ratio, and an increase in extractable nitrate in the soil and nitrate in soil solution in a study focusing on ecosystem impacts of beech bark disease.

It appears that any potential difference in soil microclimate caused by ash mortality and canopy openings in our study were insufficient to affect N turnover rates. We did observe higher rates of nitrification at the new infestation sites regardless of canopy opening compared to the old infestation sites. New infestation sites had significantly higher soil solution NO_3^- -N, inorganic-N, and total N concentrations in CG plots compared to CC plots. This initial increase in N leaching has been observed previously in studies looking at forest gaps caused by disturbances in various forest types [32,33]. Decreased plant uptake has been suggested as the primary factor contributing to the increase in N leaching [34]. However, these studies did not show the effects of gap formation on N leaching over long periods of time. At old infestation sites there was a decrease in the N concentrations in the soil solution in CG plots with an increase in time since gap formation which is coincident with the large increase in herbaceous ground vegetation N content in these plots. Herbaceous ground vegetation appears to have acted as a significant sink (via uptake) for N at the old infestation sites compared to the new infestation sites which had comparatively little herbaceous vegetation and therefore increased leaching to soil solution.

5. Conclusions

This study showed that canopy gaps resulting from the loss of ash due to EAB can lead to changes in riparian forest structure as indicated by reductions in the leaf litterfall, flux of associated nutrients to the forest floor, and growth of herbaceous ground vegetation. While N leaching was elevated during the early years after ash mortality, the establishment of herbaceous ground vegetation provided a sink for this available N and we found little evidence for an effect on soil N mineralization in forest canopy gaps. Overall, our results indicate that these transient changes resulting from the EAB-induced gap formation in riparian forests are unlikely to have strong or long-lasting effects on soil nutrient cycling.

Author Contributions: P.K.S., D.P.K., D.D and P.H. conceived and designed the experiments; D.D and P.H. performed the experiments; P.K.S, D.P.K., D.D and P.H. assisted with site set-up and sample collection; D.D. analyzed the data; P.K.S. and D.D wrote the paper; P.K.S, D.P.K., D.D and P.H. reviewed and edited the draft. All authors have read and agree to the published version of the manuscript.

Funding: This research was funded by a grant to D.P.K. and P.K.S. from The Invasive Species Center Partnership Fund, Sault Saint Marie, ON, Canada.

Acknowledgments: Jesse Harnden, Kristin Daoust, Dylan Bowes, Greg Hanta, Dain Dutkiewicz, Laura Hawdon, Linda Vogel, and Kristi Broad provided technical assistance with the field studies and laboratory sample processing.

Conflicts of Interest: The authors declare no conflict of interest.

References

- Harvey, A.E.; Geist, J.M.; McDonald, G.I.; Jurgensen, M.F.; Cochran, P.H.; Zabowski, D.; Meurisse, R.T. Biotic and Abiotic Processes in Eastside Ecosystems: The Effects of Management on Soil Properties, Processes, and Productivity. General Technical Report PNW-GTR-323; U.S. Department of Agriculture, Forest Service, Pacific Northwest Research Station: Alaska, OR, USA, 1994.
- Gandhi, K.J.K.; Herms, D.A. Direct and indirect effects of alien insect herbivores on ecological processes and interactions on forests of eastern North America. *Biol. Invas.* **2010**, *12*, 389–405. [[CrossRef](#)]
- Haack, R.A.; Jendek, E.; Liu, H.; Marchant, K.R.; Petrice, T.R.; Poland, T.M.; Ye, H. The Emerald Ash Borer: A New Exotic Pest in North America. *Newsl. Mich. Entomol. Soc.* **2002**, *47*, 1–5.
- Scarr, T.A.; McCullough, D.G.; Howse, G.A. *Agrilus planipennis*, Emerald ash borer. *For. Health Alert* **3**, 17 July 2002.
- USDA. Emerald Ash Borer. United States Department of Agriculture. 2017. Available online: <https://www.aphis.usda.gov/aphis/ourfocus/planthealth/plant-pest-and-disease-programs/pests-and-diseases/emerald-ash-borer/emerald-ash-borer> (accessed on 1 November 2017).
- Cappaert, D.; McCullough, D.G.; Poland, T.M.; Siegert, N.W. Emerald ash borer in North America: A research and regulatory challenge. *Am. Entomol.* **2005**, *51*, 122–165. [[CrossRef](#)]
- Poland, T.M.; McCullough, D.G. Emerald Ash Borer: Invasion of Urban Forest and the Threat to North American's Ash Resource. *J. For.* **2006**, *104*, 118–124.
- Nisbet, D.; Kreuzweiser, D.P.; Sibley, P.K.; Scarr, T. Ecological risks posed by emerald ash borer to riparian forest habitats: A review and problem formulation with management implications. *For. Ecol. Manag.* **2015**, *358*, 165–173. [[CrossRef](#)]
- Kreuzweiser, D.P.; Nisbet, D.; Sibley, P.K.; Scarr, T. Loss of ash trees in riparian forests from emerald ash borer infestations has implications for aquatic invertebrate leaf-litter consumers. *Can. J. For. Res.* **2019**, *49*, 134–144. [[CrossRef](#)]
- Flower, C.E.; Knight, K.S.; Gonzalez-Meler, M.A. Impacts of emerald ash borer (*Agrilus planipennis* Fiarmaire) induce ash (*Fraxinus* spp.) mortality on forest carbon cycling and successional dynamics in the eastern United States. *Biol. Invas.* **2013**, *15*, 931–944. [[CrossRef](#)]
- Matthes, J.H.; Lang, A.K.; Jevon, F.V.; Russell, S.J. Tree stress and mortality from emerald ash borer does not systematically alter short-term soil carbon flux in a mixed northeastern U.S. Forest. *Forests* **2018**, *9*, 37–53. [[CrossRef](#)]
- Kreuzweiser, D.; Dutkiewicz, D.; Sibley, P.K.; Capell, S.; Scarr, T. Changes in streamside riparian forest canopy and leaf litter nutrient flux to soils during an emerald ash borer infestation in an agricultural landscape. *Biol. Invas.* **2020**. [[CrossRef](#)]
- Engelkin, P.J.; Benbow, M.E.; McCullough, D.G. Legacy effects of emerald ash borer on riparian forest vegetation and structure. *For. Ecol. Manag.* **2020**, *457*, 117684. [[CrossRef](#)]
- Davis, J.C.; Shannon, J.P.; Van Grinsven, M.J.; Bolton, N.W.; Wagenbrenner, J.W.; Kolka, R.K.; Pypker, T.G. Nitrogen cycling responses to simulated emerald ash borer infestation in *Fraxinus nigra*-dominated wetlands. *Biogeochemistry* **2019**, *145*, 275–294. [[CrossRef](#)]
- Toczydlowski, A.J.Z.; Slesak, R.A.; Kolka, R.K.; Venterea, R.T.; D'Amato, A.W.; Palik, B.J. Effect of simulated emerald ash borer infestation on nitrogen cycling in black ash (*Fraxinus nigra*) wetlands in northern Minnesota, USA. *For. Ecol. Manag.* **2020**, *458*, 117769. [[CrossRef](#)]
- Raison, R.J.; Connell, M.J.; Khanna, P.K. Methodology for studying fluxes of soil mineral-N in situ. *Soil Biol. Biochem.* **1987**, *19*, 21–530. [[CrossRef](#)]
- Powers, R.F. Mineralizable Soil Nitrogen as an Index of Nitrogen Availability to Forest Trees 1. *Soil Sci. Soc. Am. J.* **1980**, *44*, 1314–1320. [[CrossRef](#)]
- Hazlett, P.W.; Gordon, A.M.; Voroney, R.P.; Sibley, P.K. Impact of harvesting and logging slash on nitrogen and carbon dynamics in soil from upland spruce forests in northeastern Ontario. *Soil Biol. Biochem.* **2007**, *39*, 43–57. [[CrossRef](#)]
- Kashian, D.M.; Witter, J.A. Assessing the potential for ash canopy tree replacement via current regeneration following emerald ash bore-caused mortality on southeastern Michigan landscapes. *For. Ecol. Manag.* **2011**, *261*, 480–488. [[CrossRef](#)]
- Aubin, I.; Cardou, F.; Ryall, K.; Kreuzweiser, D.; Scarr, T. Ash regeneration capacity after emerald ash borer (EAB) outbreaks: Some early results. *For. Chron.* **2015**, *91*, 291–298. [[CrossRef](#)]

21. Whitmore, T.C. Canopy gaps and the two major groups of forest trees. *Ecology* **1989**, *70*, 536–538. [[CrossRef](#)]
22. Walters, M.B.; Reich, P.B. Response of *Ulmus americana* seedlings to varying nitrogen and water status. 1 Photosynthesis and growth. *Tree Physiol.* **1989**, *5*, 159–172. [[CrossRef](#)]
23. Hausman, C.E.; Jaeger, J.F.; Rocha, O.J. Impact of the emerald ash borer (EAB) eradication and tree mortality: Potential for a secondary spread of invasive plant species. *Biol. Invas.* **2010**, *12*, 2013–2023. [[CrossRef](#)]
24. Moore, M.R.; Vankat, J.L. Responses of the herb layer to the GAP dynamics of a mature beech-maple forest. *Am. Midl. Nat.* **1986**, *115*, 336–347. [[CrossRef](#)]
25. Davis, J.C.; Shannon, J.P.; Bolton, N.W.; Kolka, R.K.; Pypker, T.G. Vegetation responses to simulated emerald ash borer infestation in *Fraxinus nigra* dominated wetlands of Upper Michigan, USA. *Can. J. For. Res.* **2017**, *47*, 319–330. [[CrossRef](#)]
26. Spies, T.A.; Franklin, J.F. Gap Characteristics and Vegetation Response in Coniferous Forests of the Pacific Northwest. *Ecology* **1989**, *70*, 543–545. [[CrossRef](#)]
27. van den Driessche, R. Prediction of mineral nutrient status of trees by foliar analysis. *Bot. Rev.* **1974**, *40*, 347–394. [[CrossRef](#)]
28. Bauhus, J.; Bartsch, N. Mechanisms for carbon and nutrient release and retention in beech forest gaps: I. microclimate, water balance and seepage water chemistry. *Plant Soil.* **1995**, *168*, 579–584. [[CrossRef](#)]
29. Jenkins, J.C.; Aber, J.D.; Canham, C.D. Hemlock woolly adelgid impacts on community structure and N cycling rates in eastern hemlock forests. *Can. J. For. Res.* **1999**, *29*, 630–645. [[CrossRef](#)]
30. Knoepp, J.D.; Vose, J.M.; Clinton, B.D.; Hunter, M.D. Hemlock infestation and mortality: Impacts on nutrient pools and cycling in Appalachian forests. *Soil Sci. Soc. Am. J.* **2011**, *75*, 1935–1945. [[CrossRef](#)]
31. Lovett, G.M.; Arthur, M.A.; Weathers, K.C.; Griffin, J.M. Long-term Changes in Forest Carbon and Nitrogen Cycling Caused by an Introduced Pest/Pathogen Complex. *Ecosystems* **2010**, *13*, 1188–1200. [[CrossRef](#)]
32. Mladenoff, D.J. Dynamics of Nitrogen Mineralization and Nitrification in Hemlock and Hardwood Treefall Gaps. *Ecology* **1987**, *68*, 1171–1180. [[CrossRef](#)]
33. Ritter, E.; Starr, M.; Vesterdal, L. Losses of nitrate from gaps of different sizes in a managed beech (*Fagus sylvatica*) forest. *Can. J. For. Res.* **2005**, *35*, 308–319. [[CrossRef](#)]
34. Scharenbroch, B.C.; Bockheim, J.G. The Effects of Gap Disturbance on Nitrogen Cycling and Retention in Late-successional Northern Hardwood–Hemlock Forests. *Biogeochemistry* **2008**, *87*, 231–245. [[CrossRef](#)]



© 2020 by the authors. Licensee MDPI, Basel, Switzerland. This article is an open access article distributed under the terms and conditions of the Creative Commons Attribution (CC BY) license (<http://creativecommons.org/licenses/by/4.0/>).